

Photoassisted mineralization of aromatic and aliphatic N-heterocycles in aqueous titanium dioxide suspensions and the fate of the nitrogen heteroatoms

Hisao Hidaka^{a,*}, Elisa García-López^{a,1},
Leonardo Palmisano^b, Nick Serpone^{c,2}

^a Frontier Research Center for the Global Environment Protection (GESC), Meisei University, 2-1-1, Hodokubo, Hino, Tokyo 191-8506, Japan

^b Dipartimento di Ingegneria Chimica dei Processi e dei Materiali, Università degli Studi di Palermo, Viale delle Scienze, 90128 Palermo, Italy

^c Dipartimento di Chimica Organica, Università di Pavia, Via Taramelli 10, Pavia 27100, Italy

Received 18 January 2007; received in revised form 13 September 2007; accepted 15 September 2007

Available online 19 September 2007

Abstract

The photoassisted degradation of aromatic heterocycles (pyrrole, imidazole, pyrazole, isoxazole, oxazole and thiazole) and N-containing alicycles (aliphatic heterocycles: pyrrolidine, 4-butanelactam and 5-pentanelactam) was examined in liquid–solid dispersions. Complete mineralization (TOC) of the aromatic heterocycles was attained within ca. 1 h of UV irradiation of the TiO₂/heterocycle system in acidic (pH 3), near-neutral (pH 6.0–7.6) and alkaline (pH 11) media. Mineralization kinetics were, in general, not appreciably influenced by the presence of acid but tended to be somewhat slower in alkaline media. N-alicycles were photomineralized more slowly than were the aromatics. The former could be mineralized in acidic and near-neutral media in less than 2 h, but not in alkaline media in which pyrrolidine, 4-butanelactam and 5-pentanelactam (and for comparison 4-butanelactone) were not mineralized even after 3 h of UV irradiation. Final products were, in all cases, CO₂, NH₄⁺ and NO₃[−] ions and SO₄^{2−} ions in the case of thiazole. Nitrogen (N₂) gas was detected only during the photooxidation of pyrazole (contains two adjacent N heteroatoms) but not imidazole in which the N atom are separated by a C atom. The molar ratio NH₄⁺/NO₃[−] depended closely on the chemical structure of the substrates at the longer irradiation times. The site and mode of adsorption of these heterocycles onto the TiO₂ particle surface were inferred from point charge calculations and the point of zero charge of the TiO₂ (pH_{pzc} ~6.7); the position of electrophilic attack by the photogenerated •OH radicals was deduced from calculated frontier electron densities.

© 2007 Elsevier B.V. All rights reserved.

Keywords: Photomineralization; Titanium dioxide; Photodegradation; N-bearing compounds; Aliphatic heterocycles; Aromatic heterocycles; Alicycles

1. Introduction

Advanced oxidation processes (AOPs) in heterogeneous media involving semiconductor metal oxides (e.g. TiO₂) are an ever growing field of basic and applied research, especially in the photooxidation of organic pollutants in aqueous media [1–3] and in the atmosphere [4–6]. AOPs offer various

advantages compared to traditional treatment methods, since reactions can be carried out at measurable rates [7] to very small concentration levels of contaminants at ambient temperatures and atmospheric pressures on irradiation in the near-UV region. Most N-containing substances are anthropogenic molecules widely employed as pesticides, herbicides and as drugs. Details of their photomineralization therefore deserve scrutiny. Azoles are heterocyclic aromatic organic molecules whose chemical structures are based on pyrrole. They form a class of five-membered heterocyclic rings with at least one other noncarbon heteroatom, e.g. nitrogen, sulfur or oxygen. They are components of larger aromatic structures that include porphyrins and the corrin ring of vitamin B12.

In the photoassisted mineralization of organic molecules containing heteroatoms such as phosphorus, sulfur and

* Corresponding author. Tel.: +81 42 591 6635; fax: +81 42 599 7785.

E-mail address: hidaka@epfc.meisei-u.ac.jp (H. Hidaka).

¹ Permanent address: Dipartimento di Ingegneria Chimica dei Processi e dei Materiali, Università degli Studi di Palermo, Viale delle Scienze, 90128 Palermo, Italy.

² Visiting Professor, Università di Pavia, Italia; Professor Emeritus, Concordia University, Montreal, Canada.

chlorine, the ultimate oxidation products are phosphate, sulfate and chloride [8], respectively. The nitrogen atoms in N-containing compounds can be converted into NO_3^- , NO_2^- and/or NH_4^+ ions. The relative amounts of these ions are closely related to the chemical structure of the initial substrates. Photooxidation of many such N-containing compounds has been carried out, with previous studies reporting either partial or complete oxidation of some amides and amines. The amine group was almost always converted to NH_4^+ ions, whereas the amount of NO_3^- produced was nearly negligible. Hydroxylated amines tend to be converted mostly into nitrate ions; the amide function is transformed into NH_4^+ ions at rates faster than for the amine functions [9].

Nitrogen-bearing surfactants also undergo complete mineralization [10]. In these structures, the water-soluble sulfonate group generates sulfate ions, whereas the primary amine moiety is converted to NH_4^+ ions and the nitro group into NO_3^- ions. Amino acids are also N-containing molecules that combine the acid function $-\text{COOH}$ and the base function $-\text{NH}_2$. Their photoassisted mineralization typically yields quantities of NH_4^+ and NO_3^- ions that depend on the structural fragment bonded to the α -carboxylic acid function [11]. Subsequent mineralization of the acid function, the nitrogen is nearly always converted to NH_4^+ ions, and to a lesser extent to NO_3^- . Only when a N–N bond is present in the original substrate is evolution of N_2 gas observed as one of the mineralization by-products. This is the case of molecules that contain hydrazo functions as present in azo-bis-formamidoacetic acid and pyridazine [12].

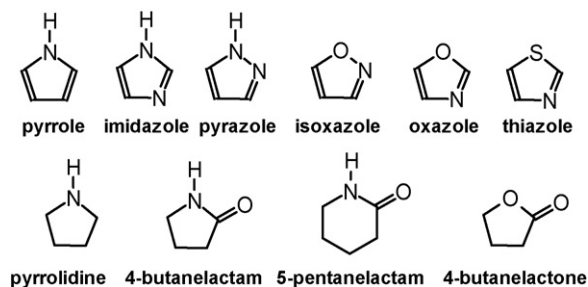
The photodegradation of formamide and urea yields NH_4^+ and NO_3^- ions as final products of nitrogen conversion, with the $\text{NH}_4^+/\text{NO}_3^-$ ratio depending on the oxidation state of the C atom to which the N heteroatom is bonded to, rather than to the oxidation state of N [13]. The C bonded to N in urea has a formal oxidation state of +4 and presents no extractable H bonded to that carbon. In this case, $\bullet\text{OH}$ radical attack occurs mainly at the $-\text{NH}_2$ function leading mostly to formation of NO_3^- ions. By contrast, when the C bonded to the N is in a lower oxidation state, as found in formamide (formally, the oxidation state of C is +2) and extractable H atoms are present, evolution of NH_4^+ ions is favored in the photoassisted process.

This study examined the photoassisted degradation of some heterocyclic aromatic and aliphatic (alicycles) molecules in a liquid–solid regime using Degussa P25 TiO_2 with the principal objectives of determining the fate of the N atom on mineralization of the substrates, and of correlating the nature of products formed with the initial molecular structure. The main products were analyzed by gas chromatography and ion chromatography; assays of inorganic carbon (IC) and total carbon (TC) levels determined the total organic carbon (TOC) present in aqueous media during the photomineralization.

2. Experimental

2.1. Chemicals and reagents

The substrates examined were the aromatic heterocycles pyrrole ($\text{C}_4\text{H}_5\text{N}$), imidazole ($\text{C}_3\text{H}_4\text{N}_2$), pyrazole ($\text{C}_3\text{H}_4\text{N}_2$),



Scheme 1. Molecular structures of aromatic (upper) and aliphatic (lower) N-heterocycles; the 4-butanelactone was examined for comparison with the 4-butanelactam.

isoxazole ($\text{C}_3\text{H}_3\text{NO}$), oxazole ($\text{C}_3\text{H}_3\text{NO}$) and thiazole ($\text{C}_3\text{H}_3\text{NS}$), and the aliphatic heterocycles pyrrolidine ($\text{C}_4\text{H}_9\text{N}$), 4-butanelactam ($\text{C}_4\text{H}_7\text{NO}$) and 5-pentanelactam ($\text{C}_5\text{H}_9\text{NO}$) and for comparison 4-butanelactone ($\text{C}_4\text{H}_6\text{O}_2$)—their structure are illustrated in Scheme 1. They were supplied by Wako Chemical Co. and used as received. Unless noted otherwise, initial concentrations of the heterocycles were 0.10 mM; the initial pH of solutions was pH 3, pH 11 or natural pH (pH ~ 6.0 to 7.6; see text below) adjusted as appropriate by addition of either HCl or NaOH. The photomediator was TiO_2 Degussa P25 (particle size, ca. 20–30 nm; specific surface area, ca. $50 \text{ m}^2 \text{ g}^{-1}$; ca. 80% anatase and $\sim 20\%$ rutile) [14].

2.2. Photoassisted degradation setup and analytical procedures

A tightly closed 127 mL Pyrex cylindrical batch photo-reactor containing 50 mL of the aqueous suspension was UV-irradiated externally with a 75-Watt medium-pressure mercury lamp (Toshiba SHL-100UVQ2; ca. 10 cm long); light irradiance $\sim 2 \text{ mW cm}^{-2}$ in the 310–400 nm range with maximal lamp emission at 360 nm (Topcon Corp. UVR-2 radiometer). The magnetically stirred suspension was purged with pure oxygen at atmospheric pressure for ca. 0.5 h prior to irradiation. The suspension temperature was maintained at ca. 313 K ($\sim 40^\circ\text{C}$) by air cooling. The loading of TiO_2 in the suspension (2 g L^{-1}) insured that all the photons from the UV light source were absorbed by the TiO_2 photomediator [15].

Temporal evolution of CO_2 and N_2 during the photoreaction was assayed by a Shimadzu GC-8AIT gas chromatograph equipped with a Shimadzu Porapack Q 80–100 column (for CO_2 analyses) or a Shimadzu Molecular sieve 5 Å 60–80 column (for N_2 analyses) and a TCD detector; helium was the carrier gas. The decrease in total organic carbon (TOC) during the photoassisted process was measured with a Shimadzu TOC-5000A analyzer and estimated as the difference between total carbon (TC) and inorganic carbon (IC). Formation of NH_4^+ , NO_2^- , NO_3^- and SO_4^{2-} ions was assayed by high-pressure liquid chromatography (Jasco; CD-5 conductivity detector; Shodex cationic (Y-521) and anionic (I-524) columns). The eluent was a 4 mM HNO_3 solution for the cationic column or a solution of phthalic acid (2.5 mM)

and tris(hydroxymethyl)aminomethane (2.3 mM) for the anionic column. Analyses were performed after separation of the photomediator by centrifugation and eventual filtration with an Advantec 0.2 μm PTFE filter. In alkaline media, the NH_3 produced (if any) was detected as NH_4^+ ions on acidification with the HNO_3 eluent during the analyses for cations.

2.3. Computer simulations

Molecular orbital calculations were performed using the paramagnetic method 3 (PM3) with application of the Window-based MOPAC program. All the geometrical parameters for the substrates examined were calculated using the Broyden–Fletcher–Goldfarb–Shannon algorithm incorporated in the program for optimization, with the minimum energy obtained at the AM1 level. Geometries of the heterocycles examined in aqueous solutions were compared with those obtained in the gas phase employing the conductor-like screening model orbital (COSMO) and electrostatic potential (point charge) calculations. The COSMO procedure generated a conducting polygonal surface around the system at van der Waal distances. Standard values used herein were the number of geometrical segments per atom (NSPA) = 60. The dielectric constant was taken as 78.4 at 25 $^\circ\text{C}$ (in water).

3. Results and discussion

3.1. TiO_2 photoassisted degradation of aromatic heterocycles

Control tests performed in the absence of TiO_2 under conditions otherwise identical to those of the TiO_2 photoassisted reactions showed no changes in TOC on samples collected up to 6 h of UV irradiation. As well, TOC measured after 3 h of stirring the substrate in the dark in TiO_2 dispersions under conditions identical to those for the photoreactions also showed no decrease, indicating that the extent of adsorption of the substrates on TiO_2 was negligible. Clearly, both TiO_2 and UV radiation are needed for degradation to occur.

The temporal changes in the levels of TOC (normalized) during the photodegradation of the aromatic heterocycles at three different initial pHs (3, 11 and near-neutral) are illustrated in Fig. 1a–f. Pyrrole was mineralized within 50 min of irradiation at pH 6.7 (Fig. 1a), whereas near-complete mineralization was achieved only after 3 h at pHs 3 and 11. Mineralization of imidazole (Fig. 1b) required about 3 h regardless of initial pH (natural pH was 7.6). Fig. 1c depicts the temporal mineralization of pyrazole attained in ca. 45 min of irradiation at pHs 3 and 6.7 (natural pH), whereas in alkaline media (pH 11) the process required longer times. In fact, only ca. 60% of pyrazole was mineralized by 50 min of UV

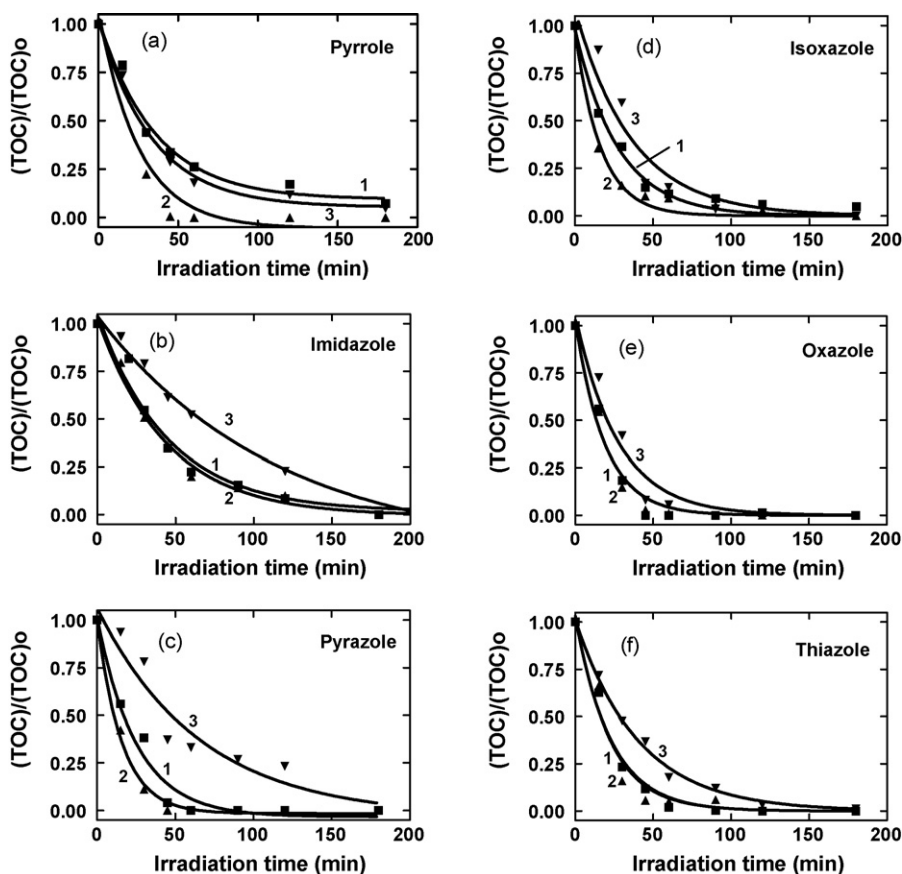


Fig. 1. Temporal changes in total organic carbon (TOC) with irradiation time for (a) pyrrole, (b) imidazole, (c) pyrazole, (d) isoxazole, (e) oxazole and (f) thiazole at pH 3 (curves 1), near-neutral pH (curves 2) and pH 11 (curves 3). Initial concentration of substrates, 0.10 mM; volume 50 mL. For initial pHs of the solutions, see text.

Table 1

Summary of kinetics of TOC decay in the liquid phase, during the photoassisted oxidation of aromatic heterocycles

Substrates	pH 3; k_{TOC} (min^{-1})	pH \sim neutral ^a ; k_{TOC} (min^{-1})	pH 11; k_{TOC} (min^{-1})
Pyrrole	0.028	0.040 (6.0) ^a	0.030
Imidazole	0.022	0.023 (7.6)	0.009
Pyrazole	0.040	0.063 (6.0)	0.015
Isoxazole	0.037	0.061 (6.8)	0.027
Oxazole	0.053	0.054 (7.6)	0.036
Thiazole	0.044	0.047 (6.5)	0.025

^a Natural pH of solutions of these heterocycles.

irradiation. Isoxazole mineralization (Fig. 1d) necessitated ca. 90 min of UV irradiation at pH 6.7. By contrast, oxazole was mineralized within 50 min at pHs 3 and 6.8 (natural pH), whereas 90 min of UV irradiation was needed to mineralize oxazole in alkaline media (pH 11; Fig. 1e). Thiazole was completely degraded within 60 min in acidic (pH 3) and neutral media (pH 6.9); the process required \sim 120 min in alkaline media (pH 11; Fig. 1f).

Consideration of the results of Fig. 1 indicates that mineralization of the aromatic heterocycles occurred in all the media examined, albeit the process was generally slower in alkaline media (see curves 3). Table 1 summarizes the relevant kinetics of mineralization of the aromatic heterocycles. In a few cases (pyrrole, pyrazole and isoxazole) mineralization was faster in neutral media than in acidic media, but no differences in k_{TOC} were seen for imidazole, oxazole and thiazole. The pH of the suspension tended to decrease somewhat after a few minutes into the photoassisted reaction, a result of the formation of H^+ and $\cdot\text{OH}$ radicals on oxidation of H_2O and/or the formation of acidic intermediates. In alkaline media, decrease in TOC levels tended to be slower than in either acid or neutral media. In all cases the decrease in TOC followed first-order kinetics.

The kinetics of TOC loss in the mineralization of aromatic N-heterocycles in neutral media (column 3; Table 1) decreased in the order: pyrazole \sim isoxazole $>$ oxazole $>$ thiazole $>$ pyrrole \gg imidazole. Heterocycles with the second heteroatom in the α -position (pyrazole and isoxazole) were mineralized faster in the first stages of photooxidation at natural pH than those with the heteroatom in the β -position (oxazole and thiazole). Imidazole with a second heteroatom also in the β -position was the slowest to be mineralized. In acidic media (pH 3) the order of mineralization was oxazole $>$ thiazole \geq pyrazole \geq isoxazole \gg pyrrole $>$ imidazole. Evidently, mineralization of substrates with the second heteroatom in the β -position were affected by H^+ (e.g. oxazole and thiazole) more so than those heterocycles with the second heteroatom in the α -position (isoxazole and pyrazole) followed by pyrrole; imidazole remained the slowest to be mineralized. In alkaline media, mineralization tended to be slower for all the heterocycles and particularly so for imidazole and pyrazole (two heterocycles whose second heteroatom is also a N atom) relative to processes in acidic and neutral media. Complete oxidation in alkaline media followed the

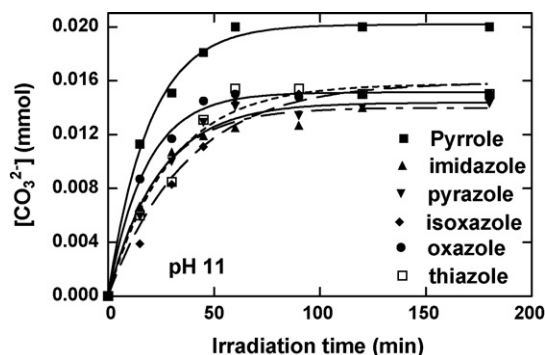
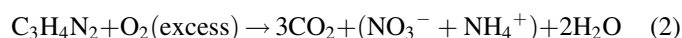
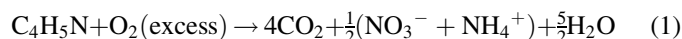


Fig. 2. Evolution of inorganic carbon as carbonate species in solution in the TiO_2 photoassisted mineralization of pyrrole, imidazole, pyrazole, isoxazole, oxazole and thiazole at pH 11. Initial concentration of the heterocycles, 0.10 mM; volume, 50 mL.

order oxazole $>$ pyrrole $>$ isoxazole \sim thiazole \gg pyrazole \gg imidazole.

Mineralization of the heterocycles was confirmed by monitoring the evolution of CO_2 by gas chromatography. Except for imidazole, the stoichiometric amounts of CO_2 evolved in acidic and neutral media were consistent with TOC assays. The kinetics of CO_2 evolution during the photoassisted degradation of all the aromatic heterocycles in acidic and neutral media were in reasonably good agreement with the kinetics of TOC decay. Although no CO_2 evolved in alkaline media, the concentration of inorganic carbon (IC) in the liquid phase for the aromatic heterocycles in the form of CO_3^{2-} species increased with irradiation time via first-order kinetics (Fig. 2): oxazole ($k_{\text{car}} = 0.056 \text{ min}^{-1}$) \geq pyrrole (0.051 min^{-1}) $>$ imidazole (0.043 min^{-1}) \sim pyrazole (0.042 min^{-1}) $>$ thiazole (0.034 min^{-1}) $>$ isoxazole (0.027 min^{-1}). Results confirm the complete mineralization of the aromatic heterocycles at pH 11 as evidenced by the quantity of IC formed in accord with expectations from the stoichiometric reactions. The case for pyrrole (4 carbon atoms) and imidazole (3 carbon atoms) are illustrated in reactions 1 and 2, respectively.



3.2. TiO_2 photoassisted degradation of aliphatic heterocycles

Fig. 3 illustrates the temporal loss of TOC during the photodegradation of the N-containing alicyclic substrates in acidic (pH 3), neutral (pH around 7) and alkaline (pH 11) media. Pyrrolidine was mineralized within \sim 120 min at pH 7.5 and at pH 3. However, in alkaline media (pH 11) TOC decay was nearly twofold slower achieving 55% mineralization after the 2 h irradiation period (see Table 2 below). Complete oxidation of 4-butanelactam (Fig. 3b) occurred within 60 min in both acidic (pH 3) and neutral (pH 6.5) media, whereas at pH 11 only 40% of the initial TOC was eliminated after 3 h of UV irradiation.

For 5-pentanelactam total mineralization occurred in ca. 90 minutes at pH 6.7 and at pH 3, whereas in alkaline pH the rate

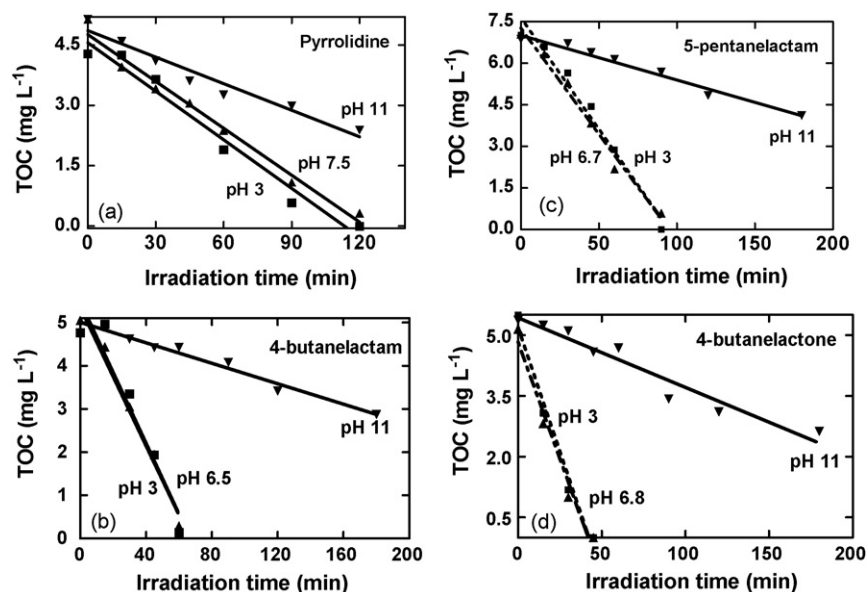


Fig. 3. Temporal evolution of total organic carbon (TOC) against irradiation time for runs carried out with (a) pyrrolidine, (b) 4-butanelactam, (c) 5-pentanelactam and (d) 4-butanelactone at pH 3, neutral pHs (see text) and pH 11.

was slower attaining only ca. 40% decrease in TOC after 3 h of irradiation (Fig. 3c). We deduce, therefore, that N-containing alicycles are completely mineralized in acidic and neutral media in less than 2 h of irradiation, whereas mineralization in alkaline media was achieved only at times longer than 3 h. Moreover, results show that N-alicycles are mineralized more slowly than aromatic heterocycles (compare Fig. 1 with Fig. 3 and Tables 1 and 2). Acid seems not to influence the kinetics of degradation of the three N-alicycles and the 4-butanelactone as evidenced by the data of Fig. 3 and Table 2 (compare data at pH 3 and pH ca. 7). By contrast, at alkaline pH the photomineralization is about 2–7 times slower for the N-alicycles and the lactone derivative, probably the result of poor adsorption of the alicycles and the lactone on the negatively charged surface of TiO₂ (point of zero charge, pH_{pzc} , ~6.7) [16] that is known to impact the degradation process. Moreover, it is well known that •OH radical addition onto aromatic substrates, in this case the heterocycles (Scheme 1), is a faster process than abstraction of a H from aliphatic substrates (e.g. the alicycles).

The photodegradation of 4-butanelactone was carried out for comparison since its structural features are similar to those of 4-butanelactam, but contains an oxygen heteroatom rather than nitrogen. Fig. 3d depicts the temporal changes of TOC decay at the three initial pHs. Mineralization at natural pH (~6.8) and pH 3 present the same pattern but faster kinetics relative to its lactam

analog, whereas the reaction was slower at pH 11 by nearly an order of magnitude. Mineralization of the O-bearing alicycle at pH 11 occurred at a rate not significantly different from the N-alicycles, whereas it degraded faster and completely to CO₂ in acidic and neutral media. Decrease in TOC content followed zero-order kinetics in all cases, contrary to the aromatic heterocycles that mineralized by first-order kinetics; relevant zero-order kinetics for the alicycles are reported in Table 2.

In near-neutral media, the mineralization rates (TOC data; Table 2) of the N-alicycles follow the order: 4-butanelactam ~ 5-pentanelactam > pyrrolidine. No doubt the presence of a carbonyl function bonded to the nitrogen heteroatom impacts on the rates of mineralization of both lactam derivatives. The slowest mineralization occurred at alkaline pH, with the order being pyrrolidine > 5-pentanelactam ≥ 4-butanelactam.

Comparison of the mineralization kinetics of aliphatic and aromatic heterocycles suggests an overall general trend for slower mineralization of the alicycles when the kinetic data of Tables 1 and 2 are compared in the same k units. In this respect, the comparison between the aromatic pyrrole and the aliphatic pyrrolidine is worth noting since they share structural similarities (see Scheme 1). Mineralization of pyrrolidine is a slower process than for pyrrole at all three pHs examined: at pH 3, $k = 0.13 \text{ mg L}^{-1} \text{ min}^{-1}$ for pyrrole versus $0.040 \text{ mg L}^{-1} \text{ min}^{-1}$ for pyrrolidine, whereas in near-neutral media

Table 2

Zero-order kinetics of TOC loss in the liquid phase in the TiO₂ photoassisted oxidation of aliphatic heterocycles

Substrates	pH 3; k_{TOC} ($10^{-2} \text{ mg L}^{-1} \text{ min}^{-1}$)	pH ~ neutral ^a ; k_{TOC} ($10^{-2} \text{ mg L}^{-1} \text{ min}^{-1}$)	pH 11; k_{TOC} ($10^{-2} \text{ mg L}^{-1} \text{ min}^{-1}$)
Pyrrolidine	4.0	3.9 (7.5) ^a	2.2
4-Butanelactam	8.2	8.0 (6.5)	1.2
5-Pentanelactam	8.0	7.6 (6.7)	1.6
4-Butanelactone	12.3	11.5 (6.8)	1.7

^a Initial natural pH of the aqueous solutions.

$k = 0.19 \text{ mg L}^{-1} \text{ min}^{-1}$ versus $0.039 \text{ mg L}^{-1} \text{ min}^{-1}$, and at pH 11 k is $0.14 \text{ mg L}^{-1} \text{ min}^{-1}$ versus $0.022 \text{ mg L}^{-1} \text{ min}^{-1}$, respectively. No doubt the faster kinetics for aromatic substrate(s) are probably due to the presence of π electrons in the aromatic (pyrrole) heterocycles that may facilitate electrophilic attack by $\bullet\text{OH}$ radicals.

The quantity of carbon dioxide evolved in acidic and neutral media with time in the gas phase during the photoassisted degradation of the three N-alicycles are in accord with the corresponding TOC decays.

3.3. Transformation of the N heteroatom into NH_4^+ and/or NO_3^- ions

3.3.1. Aromatic heterocycles

The photooxidation of aromatic and aliphatic N-heterocycles yields various ionic species with NO_3^- and NH_4^+ ions in significant quantity, along with SO_4^{2-} in the mineralization of thiazole. Nitrite ions were also detected, albeit in trace quantities, for all the substrates in photoreactions carried out in alkaline media; they were ultimately oxidized to nitrate at pH 11.

Fig. 4 illustrates the temporal evolution of NO_3^- and NH_4^+ ions produced in the oxidative photodegradation of the aromatic heterocycles. The kinetics of appearance of ammonia

($k_{\text{NH}_4^+}$) and nitrate ($k_{\text{NO}_3^-}$) along with their yields after a 3 h reaction period are summarized in Tables 3 and 4. The data also show the required induction period to observe formation of NO_3^- , along with the initial appearance of NH_4^+ ions.

The quantity of NH_4^+ ions photogenerated in acidic and near-neutral media was significantly greater than for NO_3^- in the case of pyrrole (Fig. 4a), the sum of which nearly accounted for the N mass balance after ca. 45 min into the reaction, except in alkaline media. Nitrate ions are not adsorbed on the TiO_2 surface at pHs 3–11, contrary to NH_3 for which the extent of adsorption in alkaline media (pH 11) is ca. 5% in the dark on the negatively charged TiO_2 surface [11]. This may explain (at least in part) the relatively low quantity of NH_3 (detected as NH_4^+) detected in alkaline media along with its possible oxidation to NO_3^- under these conditions (see below).

The photooxidation of imidazole, which bears a second heteroatom at the β -position, exhibits (Fig. 4b) the same behaviour as pyrrole with the photogenerated quantity of NH_4^+ significantly greater than NO_3^- species. The quantity of NO_3^- produced was slightly greater for imidazole than pyrrole. Nitrogen mass balance was attained only in acidic and neutral media.

Formation of ionic species in the photooxidation of oxazole and thiazole, that also bear a second heteroatom at

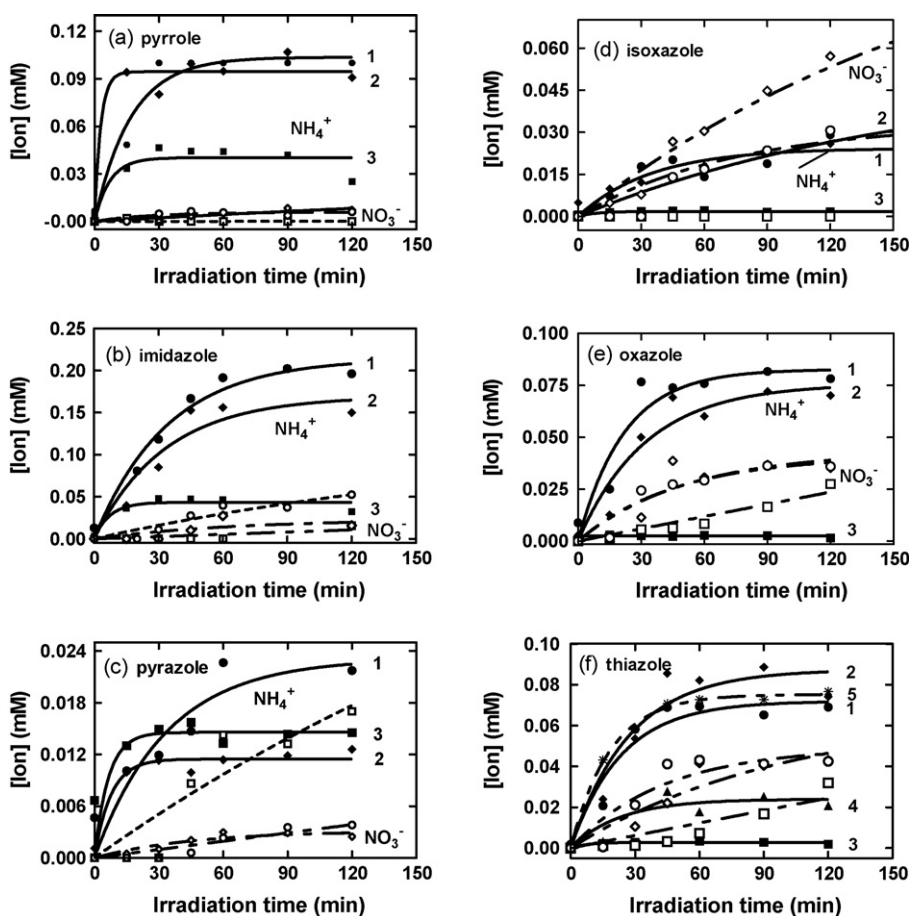


Fig. 4. Formation of NO_3^- (white symbols) and NH_4^+ (black symbols) in the photo-assisted degradation of (a) pyrrole, (b) imidazole, (c) pyrazole, (d) isoxazole, (e) oxazole and (f) thiazole at pH 3 (curves 1), neutral pH (see Tables 3 and 4; curves 2) and pH 11 (curves 3). Initial concentration, 0.10 mM; (f) also displays the temporal formation of SO_4^{2-} ions at pH ca. 6.5 (curve 4) and pH 11 (curve 5).

Table 3

Kinetics of ammonia ($k_{\text{NH}_4^+}$) and nitrate ($k_{\text{NO}_3^-}$) formation and their yields after a 3 h reaction period in the photomineralization of pyrrole, imidazole and pyrazole

Initial pH	Pyrrole			Imidazole			Pyrazole		
	3	6	11	3	7.6	11	3	6	11
$k_{\text{NH}_4^+}$ (min^{-1})	0.059	0.35	0.14	0.029	0.030	0.14	0.030	0.13	0.15
$k_{\text{NO}_3^-}$ (min^{-1})	0.038	0.0014	~0	0.0047	0.015	~0	0.00014	0.022	0.0032
NO_3^- time lag (min) ^a	–	–	–	15	30	90	30	30	30
NH_4^+ yield ^b (%)	94	91	26	80	85	11	20	12	13
NO_3^- yield ^b (%)	6	7	0	20	15	17	3	2	20

^a Time necessary to observe the presence of nitrate ions.^b Yield after 3 h.

Table 4

Kinetics of ammonia ($k_{\text{NH}_4^+}$), nitrate ($k_{\text{NO}_3^-}$) and sulfate ($k_{\text{SO}_4^{2-}}$) formation and their yields after a 3 h reaction period in the photomineralization of isoxazole, oxazole and thiazole

Initial pH	Isoxazole			Oxazole			Thiazole		
	3	6.8	11	3	7.5	11	3	6.5	11
$k_{\text{NH}_4^+}$ (min^{-1})	0.029	0.013	0.12	0.045	0.031	~0	0.043	1.4	0.049
$k_{\text{NO}_3^-}$ (min^{-1})	0.0061	0.0051	~0	0.022	0.020	0.00055	0.023	0.0099	0.011
NO_3^- time lag (min) ^a	30	Nil	–	15	15	30	15	15	30
$k_{\text{SO}_4^{2-}}$ (min^{-1})	–	–	–	–	–	–	Nil	0.043	0.055
NH_4^+ yield (%) ^b	23	32	2	65	65	2	60	60	2
NO_3^- yield (%) ^b	31	67	0	35	35	31	40	40	53
SO_4^{2-} yield (%) ^b	–	–	–	–	–	–	~0	22	70

^a Time necessary to observe the presence of nitrate ions.^b Yield after 3 h.

the β -position (Fig. 4e and f, respectively), followed a pattern similar to that of imidazole (Fig. 4b). The quantity of photogenerated NH_4^+ was also significantly greater than NO_3^- , except in alkaline media in which the amount of NH_4^+ was significantly low. Nitrogen mass balance was reached only in acidic and neutral media, but not at pH 11.

Evolution of ionic products in the photooxidation of substrates with the heteroatom located in the α -position (pyrazole and isoxazole) is illustrated in Fig. 4c and d, respectively. They exhibited a pattern different from aromatic heterocycles having the second heteroatom at the β -position. Nitrogen mass balance was not attained in the photodegradation of pyrazole in all the media examined considering only species containing nitrogen in the final products. For isoxazole (Fig. 4d), the quantity of NO_3^- was greater than NH_4^+ in neutral media probably because of the presence of the N–O function on its way to NO_3^- subsequent to $\bullet\text{OH}$ radical attack on the N heteroatom; nitrogen mass balance was also attained upon complete mineralization based on the sum of NO_3^- and NH_4^+ species. The amount of NH_4^+ detected in acidic media was similar to that formed in neutral media; however, the amount of NO_3^- detected was somewhat lower than expected.

There is a significant amount of NO_3^- formed during the photodegradation of pyrazole in alkaline media (Fig. 4c). Gaseous N_2 in equilibrium with the suspension was observed during the photoassisted mineralization of this heterocycle at natural and acidic media. The sum of NH_4^+ and NO_3^- ions produced along with the quantity of N_2 detected gave the expected nitrogen mass balance in these media.

An additional noteworthy observation is that in all cases NH_4^+ ion was formed immediately in the first stages of the photooxidations, whereas formation of NO_3^- necessitated an induction period before being detected, which infers a significantly different pathway in its formation relative to NH_4^+ ions.

The photodegradation of thiazole yielded SO_4^{2-} ions (Fig. 4f); however, the quantity produced was smaller than expected particularly at pH 3 at which no sulfate was detected in solution probably because it remains adsorbed on the positively charged TiO_2 surface. A control experiment carried out in the dark using 0.10 mM of Na_2SO_4 showed SO_4^{2-} to be adsorbed quantitatively on TiO_2 in acidic media.

Control experiments were also carried out with NH_4Cl and NaNO_3 solutions to clarify the fate of NH_4^+ and NO_3^- ions in UV-irradiated TiO_2 suspensions. Results revealed no change in the concentration of NO_3^- even after 10 h of irradiation in acidic, neutral and alkaline media. No change in NH_4^+ ion concentration occurred at pH 3 (NH_4^+) and 9 (NH_3), but decreased considerably at pH 11. Fig. 5 summarizes the temporal changes in NH_3 (detected as NH_4^+) concentration in alkaline media. The first-order decrease in NH_3 was followed by an increase in the concentration of NO_2^- and NO_3^- species, thus demonstrating conclusively that in alkaline media NH_3 is oxidized quantitatively to NO_2^- and NO_3^- after fairly long irradiation times, in accord with the work of Pollema et al. [17].

In summary, with the exception of isoxazole, the quantity of NH_4^+ produced was nearly always greater than that of NO_3^- , and the rates of formation of the latter were always significantly

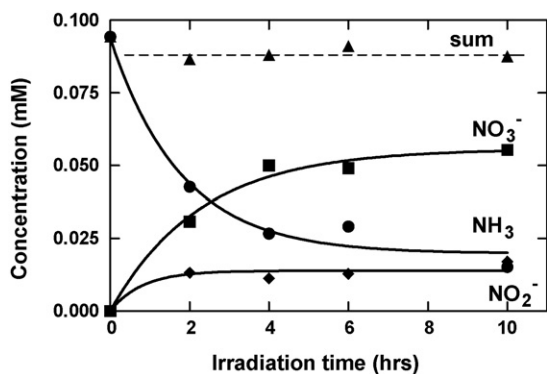


Fig. 5. Temporal changes in the concentration of NH_3 and formation of NO_3^- and NO_2^- ions during the photooxidation of NH_3 at pH 11 in the presence of TiO_2 (loading, 2 g L^{-1}). Initial concentration of NH_4Cl , 0.10 mM . The N mass balance is also displayed.

slower compared with the rates of mineralization of the substrates (k_{TOC} ; Table 1), indicating the presence of N-containing intermediates prior to complete conversion to NH_4^+ (Tables 3 and 4). The induction period for the appearance of NO_3^- and the slower rates of formation imply that nitrates are likely formed in a more complex process. Isoxazole with its N–O function in the ring (Scheme 1) is the only substrate that yielded mostly NO_3^- ions. Formation of NH_4^+ in the degradation of aromatic heterocycles depends neither on the oxidation state of N nor on the oxidation state of the C atom linked to nitrogen.

3.3.2. Aliphatic heterocycles

The temporal evolution of NH_4^+ and NO_3^- ions produced in the course of the photoassisted degradation of N-alicyclics is illustrated in Fig. 6. The photogenerated quantity of NH_4^+ in acidic and neutral media was significantly greater than NO_3^- .

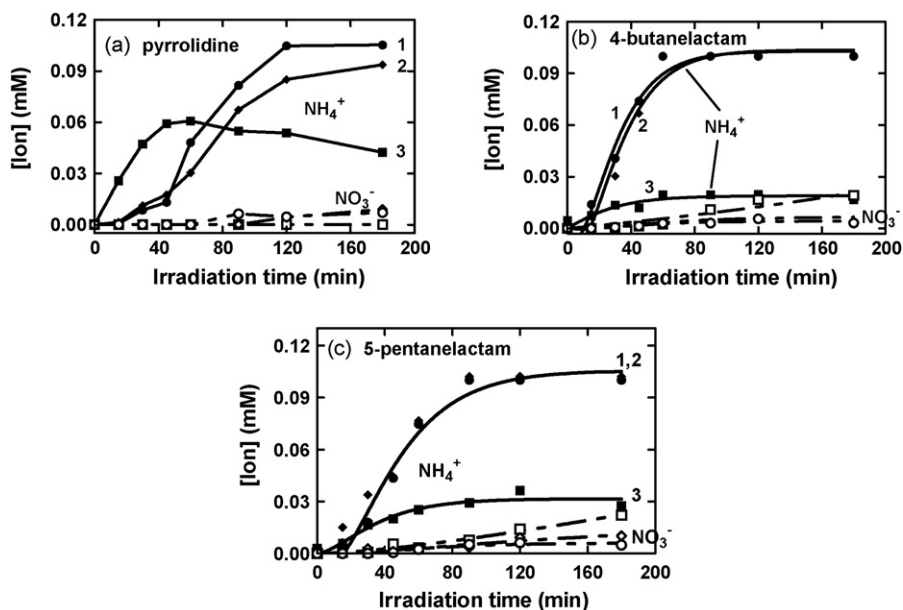


Fig. 6. Temporal evolution of NO_3^- (white symbols) and NH_4^+ (black symbols) during the photo-assisted degradation of (a) pyrrolidine, (b) 4-butanellactam and (c) 5-pentanelactam at pH 3 (curves 1); natural pH (see Table 5 for the pH; curves 2) and pH 11 (curves 3; data refer to NH_3 produced but detected as NH_4^+). Initial concentrations, 0.10 mM .

The mass balance in nitrogen is fulfilled for the photoassisted mineralization of the three N-alicyclic substrates. Degradations carried out in alkaline media showed a lesser amount of NH_3 formed which impinged on the nitrogen mass balance, due to incomplete mineralization of the alicycles, particularly those of pyrrolidine and 4-butanellactam.

The initial rates of appearance of ammonia ($r_{\text{NH}_4^+}$) and nitrate ($r_{\text{NO}_3^-}$) species along with their yields after 3 h of UV irradiation of the respective TiO_2 dispersions are summarized in Table 5. As for the aromatic heterocycles, the kinetics of appearance of NH_4^+ ions for N-containing alicycles are nearly tenfold faster than for NO_3^- ions, but somewhat slower with respect to mineralization. The only exception occurred in alkaline media (pH 11) for pyrrolidine in which the rates of formation of NH_3 was significantly faster than mineralization. This infers a possible occurrence of two different pathways for the evolution of N-containing species and the formation of organic compounds devoid of a N atom. Note that it was not the goal of this study nor was any attempt made to examine the mechanistic details of the degradation process.

3.4. Point charge and electron density calculations

The initial positions of $\bullet\text{OH}$ radical attack can be deduced from electron densities, whereas possible modes of closest approach and adsorption of the heterocycles on the TiO_2 particle surface can be inferred from calculated point charges [18–20]. An electrophilic reaction is expected to occur preferentially at a negatively charged position, whereas a nucleophilic process should take place at a positively charged position. The electrophilic position(s) in the heterocycles is that which bears the largest HOMO orbital coefficient, whereas the nucleophilic position(s) is the one with the largest LUMO orbital coefficient.

Table 5

Initial rates of formation of ammonia ($r_{\text{NH}_4^+}$) and nitrate ($r_{\text{NO}_3^-}$) along with their yields after 3 h of irradiation in the photomineralization of N-bearing alicyclic compounds

Initial pH	Pyrrolidine			4-Butanelactam			5-Pentanelactam		
	3	7.5	11	3	6.5	11	3	6.7	11
$r_{\text{NH}_4^+}^a$	1.6	2.1	67	3.7	7.2	0.36	6.0	6.0	2.0
$r_{\text{NO}_3^-}^a$	~0	~0	~0	0.24	2.9	0.24	0.42	0.18	0.24
NH_4^+ yield (%) ^b	95	95	40	97	95	17	95	90	27
NO_3^- yield (%) ^b	5	5	0	3	5	19	5	10	22

^a Rate units as (10^{-4} mM min⁻¹).

^b Yield after 3 h.

Calculated point charges and electron densities for all non-hydrogen atoms in the aromatic and aliphatic heterocycles in the gas and aqueous phases are reported in Tables 6 and 7, respectively.

When the photoreaction is carried out at an initial acid pH the TiO₂ particle surface is positively charged (partially at natural pH; see above). Consequently, the atoms that approach

more closely the metal-oxide surface will be those that bear the greatest negative point charge. Considering the structures depicted in Scheme 1 and Table 6, the most negative point charges in the symmetrical pyrrole molecule are on the C2 and C3 carbon atoms, whereas for imidazole, isoxazole and oxazole molecules it is the C2 carbons that are most negative, and for pyrazole the C3 carbon. Thiazole should be adsorbed

Table 6

Molecular orbital calculations of electron densities and point charges for the aromatic heterocycles examined in the gas phase and in aqueous solution

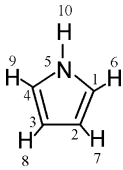
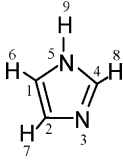
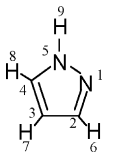
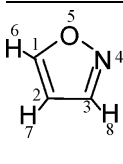
Pyrrole	Atom number	Type of atom	Point charge		Electron density	
			Gas	Water	Gas	Water
	1	C	-0.1455	-0.1689	4.1456	4.1689
	2	C	-0.1964	-0.3101	4.1964	4.3101
	3	C	-0.1964	-0.3101	4.1964	4.3101
	4	C	-0.1456	-0.1702	4.1456	4.1702
	5	N	-0.1808	-0.1391	5.1808	5.1391
Imidazole	Atom number	Type of atom	Point charge		Electron density	
			Gas	Water	Gas	Water
	1	C	-0.1717	-0.1702	4.1717	4.1702
	2	C	-0.1743	-0.2661	4.1743	4.2661
	3	N	-0.1406	-0.3499	5.1406	5.3499
	4	C	-0.1065	-0.0881	4.1065	4.0881
	5	N	-0.2084	-0.1518	5.2084	5.1518
Pyrazole	Atom number	Type of atom	Point charge		Electron density	
			Gas	Water	Gas	Water
	1	N	-0.0852	-0.2425	5.0852	5.2425
	2	C	-0.1745	-0.1918	4.1745	4.1919
	3	C	-0.2322	-0.3393	4.2322	4.3393
	4	C	-0.1264	-0.0960	4.1264	4.0960
	5	N	-0.1693	-0.1209	5.1693	5.1209
Isoxazole	Atom number	Type of atom	Point charge		Electron density	
			Gas	Water	Gas	Water
	1	C	-0.0821	-0.0064	4.0820	4.0064
	2	C	-0.2329	-0.2940	4.2329	4.2940
	3	C	-0.1646	-0.0860	4.1646	4.0860
	4	N	-0.0214	-0.1844	5.0214	5.1844
	5	O	-0.0657	-0.1422	6.0657	6.1422

Table 6 (Continued)

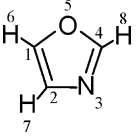
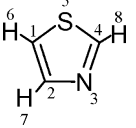
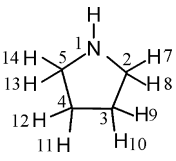
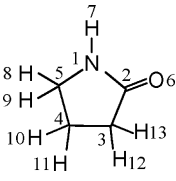
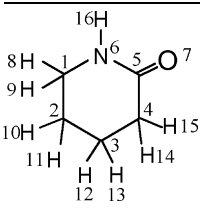
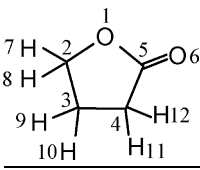
Oxazole	Atom number	Type of atom	Point charge		Electron density	
			Gas	Water	Gas	Water
	1	C	−0.1202	−0.0984	4.1202	4.0984
	2	C	−0.1746	−0.2176	4.1746	4.2176
	3	N	−0.1424	−0.3219	5.1424	5.3219
	4	C	−0.0539	0.0359	4.0539	3.9641
	5	O	−0.1277	−0.1782	6.1277	6.1782
Thiazole	Atom number	Type of atom	Point charge		Electron density	
			Gas	Water	Gas	Water
	1	C	−0.4527	−0.5630	4.4527	4.5630
	2	C	−0.1384	−0.1931	4.1384	4.1932
	3	N	−0.1019	−0.2922	5.1019	5.2922
	4	C	−0.3453	−0.4528	4.3453	4.4528
	5	S	0.4831	0.8493	5.5169	5.1507

Table 7

Molecular orbital calculation of electron densities and point charges for the aliphatic heterocycles examined in the gas phase and in aqueous solution.

Pyrrolidine	Atom number	Type of atom	Point charge		Electron density	
			Gas	Water	Gas	Water
	1	N	−0.0650	−0.1639	5.0650	5.1639
	2	C	−0.0891	−0.0924	4.0891	4.0924
	3	C	−0.1161	−0.1236	4.1161	4.1236
	4	C	−0.1131	−0.1235	4.1131	4.1235
	5	C	−0.0885	−0.0938	4.0885	4.0938
4-Butanelactam	Atom number	Type of atom	Point charge		Electron density	
			Gas	Water	Gas	Water
	1	N	−0.0684	0.1266	5.0684	4.8734
	2	C	−0.0612	−0.0924	4.0612	4.0924
	3	C	−0.1039	−0.1128	4.1039	4.1128
	4	C	−0.1239	−0.1281	4.1239	4.1281
	5	C	0.2503	0.2685	3.7497	3.7315
	6	O	−0.3791	−0.6928	6.3791	6.6928
5-Pentanelactam	Atom number	Type of atom	Point charge		Electron density	
			Gas	Water	Gas	Water
	1	C	−0.0716	−0.0919	4.0716	4.0919
	2	C	−0.1067	−0.1185	4.1067	4.1185
	3	C	−0.9546	−0.1013	4.0955	4.1013
	4	C	−0.1157	−0.1206	4.1157	4.1206
	5	C	0.2393	0.2811	3.7607	3.7189
	6	N	−0.04801	0.1180	5.0480	4.8820
	7	O	0.3722	−0.7059	6.3722	6.7059
4-Butanelactone	Atom number	Type of atom	Point charge		Electron density	
			Gas	Water	Gas	Water
	1	O	−0.2408	−0.3064	6.2408	6.3064
	2	C	0.05262	0.0675	3.9474	3.9325
	3	C	−0.1290	−0.1276	4.1290	4.1276
	4	C	−0.1300	−0.1200	4.1300	4.1201
	5	C	0.3599	0.5053	3.6400	3.4947
	6	O	−0.3269	−0.5543	6.3269	6.5543

predominantly through the C1 carbon. We deduce that the heteroatom present in the aromatic ring is not the adsorbing point, but nonetheless will be located close to the charged surface.

In alkaline media, in which the TiO_2 surface is negatively charged, the atoms approaching most closely the surface will be those with the more positive point charges in the ring structure. For pyrrole it is the N atom, whereas for imidazole it is the C4 carbon as is the case for oxazole and pyrazole; for isoxazole it is the C1 carbon. Thiazole should adsorb to the surface predominantly through the S atom. The ring is generally not expected to lie parallel to the TiO_2 surface but should tend to be perpendicular to the surface considering the point charges in aqueous media. It is noteworthy that the negative charges of the atoms constituting the heterocycles are always more negative in aqueous media than they are in the gas phase.

For the aliphatic heterocycles whose structures are depicted in Scheme 1 and the computed point charges and electron densities are reported in Table 7, the symmetrical pyrrolidine should be adsorbed mostly through the N heteroatom, whereas the 4-butanolactam, 4-butanolactone and 5-pentanolactam are likely adsorbed through the carbonyl oxygen.

The electron density of each atom in the molecules considered (Tables 6 and 7) is important in photodegradation studies since it reveals the position at which the photogenerated electrophilic $\bullet\text{OH}$ radicals will more likely attack the substrate. Note that the highest electron density is not necessarily coincident with the largest negative point charge. Taking pyrrole as an example, the highest electron density is located at the N atom. Imidazole and pyrazole contain two N atoms, one with a lone pair and the other bonded to H. In both cases, the N heteroatom with the lone pair (N3 for imidazole and N1 for pyrazole) display the maximal electron density followed by the N bonded to H. Isoxazole and oxazole bear one O and one N heteroatom. In both cases, the oxygen shows the highest electron density followed by N. Thiazole exhibits the maximal electron density at the N heteroatom followed by the S atom. We therefore deduce that the heteroatoms were the sites most likely attacked by the $\bullet\text{OH}$ radicals. This means that the substrate molecule will break at these points, forming some precursor intermediate (probably an amide [13]) toward formation of NH_4^+ ions.

4. Concluding remarks

Aromatic heterocycles can be mineralized fully through a heterogeneous TiO_2 photoassisted process occurring in acidic, neutral and alkaline media. The alkaline medium depressed the mineralization rate for all the substrates examined. Alicycles were completely degraded in acidic and neutral but not in alkaline aqueous media, and were mineralized more slowly than aromatic heterocycles, probably because of the presence of π electrons in the latter that facilitated electrophilic $\bullet\text{OH}$ radical attack. Final products were, in all cases, CO_2 , NH_4^+ and NO_3^- ions; SO_4^{2-} ions in the case of thiazole. Nitrogen gas was detected only during the photooxidation of pyrazole. The molar ratio $\text{NH}_4^+/\text{NO}_3^-$ after 3 h of irradiation was closely dependent

on the chemical structure of the substrates; however, the quantity of NH_4^+ was in nearly all cases significantly greater than NO_3^- regardless of the oxidation state of the N atom and of the C adjacent to N. Mineralization of isoxazole produced mostly NO_3^- probably because of the presence of the N–O function. The rates of appearance of N-containing species were in all cases slower than mineralization, suggesting the possible formation of some N-containing organic intermediates. Ammonium ions formed almost immediately during the first few stages of the photoreaction, whereas formation of NO_3^- necessitated an induction period inferring a more complicated pathway for its formation.

Theoretical point charge calculations suggest that the ring of the N-heterocycles is not likely oriented parallel to the TiO_2 surface and that in some cases (see Tables 6 and 7) the heteroatoms in the aromatic or alicyclic rings are not necessarily the points of contact between the heterocycles and the metal-oxide photomediator. In the case of pyrrolidine, oxazole and thiazole we cannot preclude the orientation of the rings to be nearly parallel to the metal-oxide particle surface because of the presence of three ring atoms whose negative point charges are of approximately the same magnitude. Electron density calculations suggest that the N-containing molecules will likely cleave, subsequent to $\bullet\text{OH}$ radical attack, at the points where the heteroatoms are located.

Acknowledgements

Our work in Tokyo was sponsored by the Ministry of Education, Culture and Sports, Science and Technology of Japan (Grand-in-aid for Scientific Research No. 17550145 to HH). One of us (NS) is grateful to Prof. Albini of the University of Pavia for his kind hospitality. We also gratefully acknowledge the assistance of Prof. T. Kurihara and Ms. T. Ohno (Josai University) for the molecular orbital simulations.

References

- [1] M. Schiavello (Ed.), *Heterogeneous Photocatalysis*, John Wiley & Sons, New York, 1995.
- [2] N. Serpone, Pelizzetti F. E. (Eds.), *Photocatalysis. Fundamentals and Applications*, John Wiley & Sons, New York, 1989.
- [3] A. Fujishima, K. Hashimoto, T. Watanabe, *TiO₂ Photocatalysis: Fundamentals and Applications*, Bkc, Tokyo, 1999.
- [4] A. Augugliaro, S. Coluccia, E. García-López, V. Loddo, G. Marcì, G. Martra, L. Palmisano, M. Schiavello, *Top. Catal.* 35 (2005) 237–244.
- [5] J. Peral, D.F. Ollis, *J. Catal.* 136 (1992) 554–565.
- [6] M.L. Sauer, D.F. Ollis, *J. Catal.* 158 (1996) 570–582.
- [7] A.L. Linsebigler, G. Lu, J.T. Yates Jr., *Chem. Rev.* 95 (1995) 735–758.
- [8] C.S. Turchi, D.F. Ollis, *J. Catal.* 122 (1990) 178–194.
- [9] K. Nohara, H. Hidaka, E. Pelizzetti, N. Serpone, *J. Photochem. Photobiol. A: Chem.* 102 (1997) 265–272 (and references therein).
- [10] H. Hidaka, K. Nohara, J. Zhao, E. Pelizzetti, N. Serpone, *J. Photochem. Photobiol. A: Chem.* 91 (1995) 145–152.
- [11] S. Horikoshi, N. Serpone, J. Zhao, H. Hidaka, *J. Photochem. Photobiol. A: Chem.* 118 (1998) 123–129 (and references therein).
- [12] S. Horikoshi, H. Hidaka, *J. Photochem. Photobiol. A: Chem.* 141 (2001) 201–207 (and references therein).
- [13] E. Pelizzetti, P. Calza, G. Mariella, V. Maurino, C. Minero, H. Hidaka, *Chem. Commun.* (2004) 1504–1505 (and references therein).

- [14] S. Horikoshi, N. Serpone, J. Zhao, H. Hidaka, J. Photochem. Photobiol. A: Chem. 118 (1998) 123–129.
- [15] A. Salinaro, A.V. Emeline, J. Zhao, H. Hidaka, V.K. Ryabchuk, N. Serpone, Pure Appl. Chem. 71 (1999) 321–335.
- [16] N. Watanabe, S. Horikoshi, H. Hidaka, N. Serpone, J. Photochem. Photobiol. A: Chem. 174 (2005) 229–238.
- [17] C.H. Pollema, E.B. Milosavljević, J.L. Hendrix, L. Solujić, H. Nelson, Monatshefte Chem. 123 (1992) 333–339.
- [18] M.J.S. Dewar, E.G. Zebisch, E.F. Healy, J.J.P. Stewart, J. Am. Chem. Soc. 107 (1985) 3902–3909.
- [19] M.J.S. Dejar, Y.C. Yuan, Inorg. Chem. 29 (1990) 3881–3890.
- [20] J.J.P. Stewart, J. Comp. Chem. 10 (1989) 209–220.